Fluorescence quenching by a metal nanoparticle in the extreme near-field regime

E. Castanié,[1] M. Boffety,[1,2] and R. Carminati[1,*]

[1]Institut Langevin, ESPCI ParisTech, CNRS UMR 7587, 10 rue Vauquelin, 75231 Paris CEDEX 05, France
[2]Laboratoire EM2C, Ecole Centrale Paris, CNRS UPR 288, 92295 Châtenay-Malabry CEDEX, France
*Corresponding author: remi.carminati@espci.fr

Received October 20, 2009; revised December 10, 2009; accepted December 21, 2009;
posted December 23, 2009 (Doc. ID 118810); published January 22, 2010

We study the spontaneous decay rate of a dipole emitter close to a metallic nanoparticle in the extreme near-field regime. The metal is modeled using a nonlocal dielectric function that accounts for the microscopic length scales of the free electron gas. We describe quantitatively the crossover between the macroscopic and microscopic regimes and the enhanced nonradiative decay due to microscopic interactions. Our theory is in agreement with results previously established in the asymptotic near- and far-field regimes. © 2010 Optical Society of America

OCIS codes: 260.2510, 260.2160, 160.4236, 290.5850.

The controlled modification of spontaneous emission is a central issue in photonics. Modifications of the spontaneous decay rate of molecules close to metallic surfaces [1] or atoms in cavities [2] have become textbook examples. The development of nano-optics techniques has stimulated the use of metallic nanoparticles or tips to act on the excited-state lifetime [3], on the fluorescence intensity [3,4], and on the radiation pattern [5,6] of isolated emitters, leading to the concept of optical nanoantenna. The interplay among the enhancement of the excitation intensity, nonradiative decay, and changes in the radiation pattern [7,8] offers useful degrees of freedom. Fluorescence enhancement can be optimized for imaging applications or single photon sources, while efficient quenchers can be designed for biochemical applications [9,10].

In this Letter we study quantitatively the spontaneous decay rate of a single emitter coupled to a metallic nanoparticle, up to a regime in which the macroscopic description of the electrodynamics of the metal surface breaks down. This regime is expected when the distance to the metal surface is on the order of the microscopic length scales driving the electron dynamics. In this regime, the metal surface has to be described using a spatially nonlocal dielectric function. In the context of molecular fluorescence, a general formalism and the main trends have been described by Ford and Weber [11]. More recently, a giant enhancement of the nonradiative decay rate due to microscopic interactions at a plane metal surface has been predicted [12], and a simplified nonlocal model has been used to describe the change in the radiative and nonradiative decay rates of molecules adsorbed on small nanoparticles [13]. In the present study, we describe the full crossover between the far-field regime and the extreme near-field regime (up to physical contact) in the case of nanoparticles with size R satisfying $\ell < R \ll \lambda$, where ℓ is the electron mean free path and λ is the emission wavelength. Note that this condition does not include the case of very small particles ($R < 10$ nm) [13,14] in which other mechanisms, such as quantum confinement, can be involved. Handling the full emitter-nanoparticle distance range requires a more sophisticated model than that used in [12,13] and allows us to determine precisely the breakdown of the macroscopic approach, thus providing an answer to a recurrent issue in nano-optics [15].

In the weak-coupling regime, the spontaneous decay rate of a dipole emitter located at position $\mathbf{r}$ takes the form $\Gamma = (2/\hbar)|\mathbf{p}|^2 \mathrm{Im}[\mathbf{u}\cdot\mathbf{G}(\mathbf{r},\mathbf{r},\omega)\cdot\mathbf{u}]$, where $\mathbf{p}$ is the transition dipole, $\mathbf{u} = \mathbf{p}/|\mathbf{p}|$, and ω is the emission frequency [16]. The dyadic Green's function $\mathbf{G}$ describes the electrodynamic response of the environment. It connects an electric dipole at position $\mathbf{r}$ to the radiated electric field at position $\mathbf{r}'$ through the relation $\mathbf{E}(\mathbf{r}',\omega) = \mathbf{G}(\mathbf{r}',\mathbf{r},\omega)\cdot\mathbf{p}$. In free space, the decay rate is obtained from the vacuum Green's function and reads $\Gamma_0 = \omega^3|\mathbf{p}|^2/(3\pi\epsilon_0\hbar c^3)$.

For a single emitter interacting with a spherical nanoparticle, $\mathbf{G}$ can be computed using the Mie series [17]. The decay rate obtained with this approach is shown in Fig. 1 (blue solid line) versus the distance z between the emitter and the surface of a silver nanoparticle with radius of $R = 25$ nm. The bulk value of

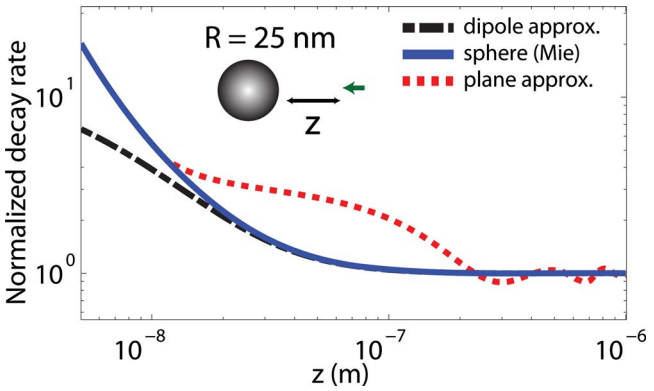

Fig. 1. (Color online) Normalized decay rate Γ/Γ_0 close to a silver sphere ($R = 25$ nm) versus the distance z between the emitter and the sphere surface. Emission wavelength $\lambda = 700$ nm. The nanoparticle is described by a local (bulk) dielectric function with three different models: electric dipole model (black dashed line), Mie theory (blue solid line), and plane model (red dotted line).

the dielectric function of silver is used, with $\epsilon = -24.2 + 0.91i$ at the emission wavelength of $\lambda = 700$ nm [11]. One can identify three regimes. For small particles ($R \ll \lambda$) and large distances ($z \gg R$), the electric dipole approximation can be used [18]. The result obtained with this approximation is plotted in Fig. 1 (black dashed line) and is in agreement with the exact Mie calculation for $z > 2R$. For very short distances ($z \ll R$), the nanoparticle can be modeled by a semi-infinite medium with a plane interface. The result obtained in the plane approximation is plotted in Fig. 1 (red dotted line), and the calculations for the sphere and for the plane coincide for $z < 12$ nm (i.e., $z < R/2$). In this regime, the decay rate exhibits a z^{-3} power law dependence, which is a well-known result in the macroscopic theory [1]. In the intermediate regime ($20 < z < 200$ nm), the decay rate obtained with the (infinite) plane surface is larger than that of the nanoparticle due to a larger effective cross section, with the radiative and nonradiative decay rates being on the same order of magnitude (calculation not shown for brevity). With the nanoparticles considered in this study (with radius of $R \sim 20-100$ nm) one expects the deviation from the macroscopic description (based on bulk values of the dielectric function) for distances z on the order of the microscopic length scales driving the electron dynamics. Since these scales are on the order of 1–10 nm for noble metals, the deviations should occur in the regime $z < R/2$, where the nanoparticle behaves as a plane surface. For this reason, the microscopic theory that is developed below is limited to the case of a flat surface.

The Green's dyadic $\mathbf{G}$ is known analytically in Fourier space for a flat surface [19]. For a transition dipole oriented along the normal to the surface (z direction), the normalized decay rate reads

$$\frac{\Gamma}{\Gamma_0} = 1 + \frac{3}{2\epsilon_1 k_0^3}\mathrm{Re}\int_0^\infty \frac{K^3}{q_1(K)} r_p(K)\exp[2iq_1(K)z]\mathrm{d}K. \tag{1}$$

In this expression $k_0 = \omega/c$, ϵ_1 is the dielectric function of the medium surrounding the emitter, $q_1(K) = (\epsilon_1 k_0^2 - K^2)^{1/2}$ with the determination $\mathrm{Im}\, q_1(K) > 0$, and $r_p(K)$ is the Fresnel reflection factor for p polarization at the metal interface (this is the only polarization involved for a dipole emitter oriented along the z direction). When the distance z becomes comparable to (or smaller than) the microscopic length scales describing the electron dynamics, the response of the metal differs from that of the bulk material. First, the dielectric function becomes spatially nonlocal or wavevector dependent in Fourier space (one refers to spatial dispersion, by analogy with frequency dispersion which corresponds to nonlocality in the time domain). We use the Lindhardt–Mermin (LM) model, described in [11] and used recently to model nanoscale radiative heat transfer [20,21]. Second, the microscopic behavior of the electron gas at the interface has to be handled. In the infinite barrier model, in which electrons at the surface undergo specular reflection, the Fresnel reflection factor can be written in terms of a surface impedance $Z(K)$ [11],

$$r_p(K) = \frac{q_1(K)/(\omega\epsilon_1) - Z(K)}{q_1(K)/(\omega\epsilon_1) + Z(K)}. \tag{2}$$

The surface impedance depends on the transverse and longitudinal components of the nonlocal dielectric function of the metal,

$$Z(K) = \frac{2i}{\pi\omega}\int_0^\infty \left[\frac{q^2}{\epsilon_t(k,\omega) - (k/k_0)^2} + \frac{K^2}{\epsilon_l(k,\omega)}\right]\frac{\mathrm{d}q}{k^2}, \tag{3}$$

with $k^2 = K^2 + q^2$. In the LM model, the longitudinal and transverse dielectric functions read

$$\epsilon_l(k,\omega) = \epsilon_b + \frac{3\omega_p^2}{\omega + i\nu}\frac{u^2 f_l(a,u)}{\omega + i\nu f_l(a,u)/f_l(a,0)}, \tag{4}$$

$$\epsilon_t(k,\omega) = \epsilon_b - \frac{\omega_p^2}{\omega^2(\omega + i\nu)}\{\omega[f_t(a,u) - 3a^2 f_l(a,u)] + i\nu[f_t(a,0) - 3a^2 f_l(a,0)]\}, \tag{5}$$

where ω_p is the plasma frequency and ν is the electron collision rate. The constant ϵ_b is an effective parameter accounting for interband transitions, as in the classical Drude model (the latter being recovered at large scales or small k). The arguments $a = k/(2k_F)$ and $u = (\omega + i\nu)/(kv_F)$, with k_F and v_F being the Fermi wavevector and velocity, contain the relevant microscopic length scales: the electron mean free path $\ell = v_F/\nu$, the distance $\delta = v_F/\omega$ traveled by an electron during one period of the electromagnetic field, and the Fermi wavelength $\lambda_F = 2\pi/k_F$. The functions $f_l(a,u)$ and $f_t(a,u)$ are given in [11,21] and are summarized as a note for completeness [22]. The model includes the mechanism of Landau damping, i.e., absorption of photons by accelerated free electrons in the regime $k\delta > 1$ that was described previously in [12]. We stress that the use of the full LM model with both longitudinal and transverse dielectric functions is necessary in order to describe continuously the transition to the macroscopic approach when z increases, as well as the influence of the electron mean free path.

We show in Fig. 2 the normalized decay rate for a flat surface of silver, computed using the local (red dotted line) and the nonlocal (blue solid line) models at a wavelength of $\lambda = 700$ nm. At short distance, the decay rate increases in both cases due to nonradiative coupling (the radiative decay rate is negligible). The slope is larger in the nonlocal model than predicted by the macroscopic theory due to nonradiative coupling to free electrons on scales smaller that the mean free path. For $z = 1$ nm, the decay rate computed with the microscopic approach is eight times larger. The deviation starts for $z \lesssim \ell$ ($\ell = v_F/\nu = 16$ nm for silver), which sets the onset of the breakdown of the macroscopic approach. At such distances, the quasi-static approximation is accurate as shown in the inset in Fig. 2 and allows one to compute approximate expressions. The macroscopic approach predicts $\Gamma \sim z^{-3}$. In the regime $z \sim \delta \ll \ell$, where the Landau

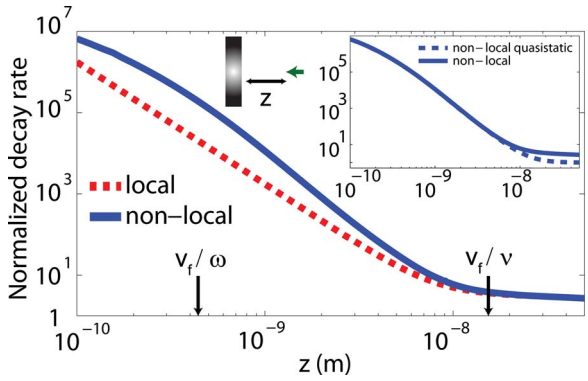

Fig. 2. (Color online) Normalized decay rate Γ/Γ_0 in the extreme near-field regime for a silver plane. Emission wavelength $\lambda = 700$ nm. Red dotted line, bulk dielectric function. Blue solid line, nonlocal model with parameters $\epsilon_b = 3.6$, $\omega_p = 1.42 \times 10^{16}$ s^{-1}, and $\nu = 8.79 \times 10^{13}$ s^{-1} [11]. The relevant length scales are indicated on the horizontal axis. Inset, comparison between the quasi-static approximation and the full calculation using the nonlocal model.

damping is expected to dominate, the microscopic approach predicts $\Gamma \sim z^{-4}$ [12], which is in good agreement with the slope given by the full calculation in Fig. 2. Finally, we note that, for $z \lesssim 0.5$ nm, the onset of a saturation of the decay rate is observed. Indeed, for wavevectors $k > k_F$, the model predicts a reduced absorption due to a sharp cutoff in the imaginary part of the dielectric function [21]. Although this saturation is expected physically at some point, a precise computation in this region would require a more refined model, including an atomic description of the interface.

We have given a framework for the calculation of the spontaneous decay rate from the extreme (microscopic) near-field regime to the far-field (macroscopic) regime, with a full description of the crossover (the blue solid curves in Figs. 1 and 2 can be continuously connected). For nanoparticles satisfying $R > l$, the electron mean free path ℓ has been confirmed as the critical distance below which the macroscopic description breaks down. In the regime $z \ll R$, the nonradiative decay rate dominates (quenching) and can be enhanced due to microscopic interactions. It coincides with that of a plane surface, being essentially independent on the size and shape of the nanoparticle. The enhanced nonradiative decay rate translates into the apparent quantum yield η (or the quenching efficiency $QE = 1 - \eta$). For silver and a distance of $z = 1$ nm, our calculation predicts a reduction in η by a factor of 8 compared to the value predicted by the macroscopic description. A similar but weaker trend is observed for gold at the same wavelength. For $z = 1$ nm, one obtains a reduction in η by a factor of 2. The weakness of the effects for gold, as well as a smaller mean free path ($\ell = 12$ nm), might explain the apparent robustness of macroscopic approaches in describing experimental results with gold nanoparticles for $z > 5$ nm [3,4,8].

This work was supported by the European Union (EU) project *Nanomagma* under contract NMP3-SL-2008-214107. We acknowledge C. Henkel and Vuong Thi Kim Thanh for helpful discussions. E. Castanié acknowledges a doctoral grant from the French Direction Générale de l'Armement.

References and Notes

1. R. R. Chance, A. Prock, and R. Silbey, Adv. Chem. Phys. **37**, 1 (1978).
2. P. Berman, ed., *Cavity Quantum Electrodynamics* (Academic, 1994).
3. S. Kühn, U. Hakanson, L. Rogobete, and V. Sandoghdar, Phys. Rev. Lett. **97**, 017402 (2006).
4. P. Anger, P. Bharadwaj, and L. Novotny, Phys. Rev. Lett. **96**, 113002 (2006).
5. P. Mühlschlegel, H.-J. Eisler, O. J. F. Martin, B. Hecht, and D. W. Pohl, Science **308**, 1607 (2005).
6. T. H. Taminiau, F. D. Stefani, F. B. Segerink, and N. F. van Hulst, Nature Photon. **2**, 234 (2008).
7. M. Thomas, J.-J. Greffet, R. Carminati, and J. R. Arias-Gonzales, Appl. Phys. Lett. **85**, 3863 (2004).
8. S. Kühn, G. Mori, M. Agio, and V. Sandoghdar, Mol. Phys. **106**, 893 (2008).
9. T. Pons, I. L. Medintz, K. E. Sapsford, S. Higashiya, A. F. Grimes, D. S. English, and H. Mattoussi, Nano Lett. **7**, 3157 (2007).
10. J. Seelig, K. Leslie, A. Renn, S. Kühn, V. Jacobsen, M. van de Corput, C. Wyman, and V. Sandoghdar, Nano Lett. **7**, 685 (2007).
11. G. W. Ford and W. H. Weber, Phys. Rep. **113**, 195 (1984).
12. I. A. Larkin, M. I. Stockman, M. Achermann, and V. I. Klimov, Phys. Rev. B **69**, 121403(R) (2004).
13. J. Vielma and P. T. Leung, J. Chem. Phys. **126**, 194704 (2007).
14. T. L. Jennings, M. P. Singh, and G. F. Strouse, J. Am. Chem. Soc. **128**, 5462 (2006).
15. O. Keller, Phys. Rep. **268**, 85 (1996).
16. J. M. Wylie and J. E. Sipe, Phys. Rev. A **30**, 1185 (1984).
17. H. Chew, J. Chem. Phys. **87**, 1355 (1987).
18. R. Carminati, J.-J. Greffet, C. Henkel, and J. M. Vigoureux, Opt. Commun. **261**, 368 (2006).
19. J. E. Sipe, J. Opt. Soc. Am. B **4**, 481 (1987).
20. C. Henkel and K. Joulain, Appl. Phys. B **84**, 61 (2006).
21. P. O. Chapuis, S. Volz, C. Henkel, K. Joulain, and J.-J. Greffet, Phys. Rev. B **77**, 035431 (2008).
22. The LM functions read $f_l(a,u) = 1/2 + [1 - (a-u)^2]/(8a)\ln[(a-u+1)/(a-u-1)] + [1-(a+u)^2]/(8a) \times \ln[(a+u+1)/(a+u-1)]$ and $f_t(a,u) = 3(a^2+3u^2+1)/8 - 3[1-(a-u)^2]^2/(32a)\ln[(a-u+1)/(a-u-1)] - 3[1-(a+u)^2]^2/(32a)\ln[(a+u+1)/(a+u-1)]$. The limit $u \to 0$ has to be taken with a positive imaginary part so that $\ln[(a \pm u+1)/(a \pm u-1)] \sim \ln|(a+1)/(a-1)|$.